ISSN 1340-3745

ICRR

FERMILAB
MAY 29 1996
LIBRARY

ICRR-Report-363-96-14

ICRR-363-96-14

(1) Very High Energy Emission from Pulsars

T. Kifune

Fermilab Library
0 1160 0042754 4

(2) Recent Status of Next CANGAROO Project of Air Čerenkov Imaging Telescope for sub-hundred GeV Gamma Ray Detection

CANGAROO Collaboration
presented by T. Tanimori

(April, 1996)

(1) Presented in IAU Colloquium 160, Pulsars : "Problems & Progress"
(Sydney, January 8-12, 1996)
(2) Presented in the Workshop for "Very High Energy Astrophysics"
(Fujiyoshida, December 13-16, 1995)

INSTITUTE FOR COSMIC RAY RESEARCH
UNIVERSITY OF TOKYO
3-2-1 Midori-cho, Tanashi, Tokyo 188, Japan

Very High Energy Emission from Pulsars

T. Kifune

Institute for Cosmic Ray Research, University of Tokyo, Tokyo 188, Japan

Abstract

Observations of gamma rays around 10^{12} eV (= 1 TeV) from pulsars are reviewed and the results are discussed and compared with emission at other wavelengths. Very high energy gamma rays do not appear to be modulated with the pulsar period, which suggests that a major part of the VHE emission is not from the pulsar magnetosphere.

1 Introduction

Observations of Very High Energy (VHE) gamma rays beyond 100 GeV are made using the ground-based air Čerenkov technique. The large collecting area this technique provides is necessary for detecting the small photon flux, which rapidly decreases with energy following a non-thermal power law spectrum. Recently, the detection sensitivity at VHE energies was improved, and also the angular resolution narrowed to about 0.1°, with the development of the imaging Čerenkov technique (e.g. Cawley and Weekes 1995). The pioneering success of the technique preceded by several years the launch of the Compton Gamma Ray Observatory (CGRO) in 1991. The EGRET detections of GeV gamma rays (e.g. Ramanamurthy et al. 1995, and references therein), have resulted in pulsars becoming one of the most important targets of VHE observations, diverting from 1980's attempts devoted mainly to X-ray and millisecond pulsars.

The detection of VHE gamma rays provides evidence of progenitor electrons at higher energies, accelerated by the induced electric field arising from the rapid rotation of the high magnetic field of the pulsar. A possible mechanism for radiating the VHE gamma rays is the inverse Compton process by which ambient soft photons at radio to optical wavelengths are scattered by the (>TeV) electrons and boosted to $\sim$ TeV energies. It is, however, not clear under what conditions the presence of the energetic electrons can lead to VHE gamma ray emission; the alternative process of synchrotron radiation dissipates the energy of the progenitor electrons into softer photons. Furthermore, after production, energetic gamma rays can be absorbed within the source by conversion into an electron-positron pair. The various mechanisms have been discussed

by a number of authors, and efforts made to model the complex cascade phenomena in the plasma of high energy electrons and positrons, and discern the role of the magnetic field structure near or at the pulsar (e.g. see Cheng and de Jager 1990 for a discussion of theoretical models relevant to VHE gamma rays). Observational upper limits on the flux of radiated photons at the highest energies can put useful constraints on the various emission models.

2 Observational results

2.1 Crab nebula/pulsar and other EGRET pulsars

A number of groups have now detected an excess 'DC' (i.e. unpulsed) flux from the Crab, whereas the results on the 'pulsed' signal, modulated with pulsar period, are apparently not consistent with each other (Table 1). The imaging technique is used by the Whipple, CANGAROO, HEGRA and Crimean groups. The Crab is the best studied object, but the highest energy emission detected so far is limited to $\sim$10 TeV. Observations higher than $\sim$10 TeV have produced negative results with upper limits slightly above the spectrum extrapolated from lower energies (e.g. Borione et al. 1995). The VHE data do not yet cover a sufficiently wide range of energy with good enough accuracy and statistics, and the power indices of the integral spectrum of photon number reported to date range between -1.4 and -1.7. However, when combined with the EGRET data, the global features of the Crab spectrum now allow us to argue about the identification of the origin of the target photons for the inverse Compton effect and the possible contribution of the bremsstrahlung process (Aharonian and Atoyan 1995).

CANGAROO data show evidence of unpulsed gamma rays from the directions of the Vela pulsar and PSR B 1706−44. As for Geminga, positive detections of a pulsed signal in early 1980s data have been claimed by the Durham and Tata groups. The more recent imaging Čerenkov result of the Whipple group gives an upper limit which is near the flux reported by the Tata group and is one order of magnitude smaller than the earlier result of the Durham group. For PSR 1951+32, the Whipple upper limit on the DC flux is $5.4 \times 10^{-12}\,\mathrm{cm}^{-2}\,\mathrm{s}^{-1}$ (Weekes 1996). A preliminary analysis of CANGAROO data on PSR B 1055−52 shows no evidence of detection, with an upper limit as small as $10^{-12}\,\mathrm{cm}^{-2}\,\mathrm{s}^{-1}$. No TeV observation has been reported on the newest EGRET pulsar PSR B 0656+14 (Ramanamurthy et al. 1996).

2.2 Millisecond/binary pulsars

Table 2 lists VHE observations of short period pulsars. Evidence of pulsed emission was reported for PSR B 1937+21 and for the binary pulsars, PSR B 1953+29 and 1855+09,

Table 1: Observations of the Crab, PSR B 1706−44, Vela and Geminga

Group (reference)	Flux (cm^{-2} s^{-1})	$E_{th}^{(*)}$
========== Crab ==========		
— unpulsed —		
Whipple (Lewis et al. 1993)	$8.8 \times 10^{-12}(E/TeV)^{-1.69}$	0.4
Crimea (Kalekin et al. 1995)	1.3×10^{-11}	1
ASGAT (Goret et al. 1993)	2.7×10^{-11}	0.6
HEGRA (Konopelko et al. 1995)	$8 \times 10^{-12}(E/TeV)^{-1.7}$	1
Themistocle (Djannati-Atai et al. 1995)	$2.3 \times 10^{-12}(E/3TeV)^{-1.4}$	2.3
CANGAROO (Tanimori et al. 1994)	7.6×10^{-13}	7
— pulsed —		
Whipple (Gillanders et al. 1995)	$< 2.0 \times 10^{-13}$	0.25
Gulmarg (Sapru et al. 1996)	$< 2.5 \times 10^{-12}$	4
Tata (Vishwanath et al. 1994)	$(9.7 \pm 4.3) \times 10^{-12}$	1
Durham (Dowthwaite et al. 1984)	$(7.9 \pm 1.8) \times 10^{-12}$	1
========== PSR B 1706−44 ==========		
— unpulsed —		
CANGAROO (Kifune et al. 1995)	8×10^{-12}	1
— pulsed —		
Potchefstroom (Nel et al. 1993)	$< 5.8 \times 10^{-12}$	2.6
========== Vela pulsar ==========		
— unpulsed —		
CANGAROO (in preparation)	$\sim 3 \times 10^{-12}$	~ 1
— pulsed —		
SAO/Sydney (Grindlay et al. 1975)	$< 8.5 \times 10^{-11}$	0.3
Tata(Bhat et al. 1987)	$\sim 1 \times 10^{-12}$	5
Durham(Bowden et al. 1993a)	$< 5 \times 10^{-11}$	0.3
Potchefstroom(Nel et al. 1993)	$< 6 \times 10^{-12}$	2.3
Adelaide(Edwards et al. 1994)	$< 7 \times 10^{-11}$	0.8
========== Geminga ==========		
— unpulsed —		
Whipple(Akerlof et al. 1993)	$< 8.9 \times 10^{-12}$	0.5
— pulsed —		
Durham(Bowden et al. 1993b)	3×10^{-11}	1
Tata(Vishwanath et al. 1993)	$(2.1 \pm 0.8) \times 10^{-11}$	0.8
	$(4.4 \pm 3.5) \times 10^{-12}$	1.7
Whipple(Akerlof et al. 1993)	$< 5 \times 10^{-12}$	0.5

(*) : Threshold energy of detected gamma ray in TeV.

by the Durham group (Bowden et al. 1990; Chadwick et al. 1985). The Potchefstroom group saw evidence of emission from PSR B 1855+09 (Brink et al. 1990), but an upper limit on the DC flux (irrespective of pulsed or unpulsed emission) obtained by Whipple group (Reynolds et al. 1993) is smaller than the flux of the positive detection reported. A hint of emission was reported also on PSR B 1957+20, a binary pulsar with a 1.6 ms period, by the Potchefstroom group, but a later observation by the same group failed to reconfirm this (Brink et al. 1993). The upper limit of Durham group is smaller than the Potchefstroom flux. In a summary of Potchefstroom observations (Nel et al. 1992), the two pulsars PSR B 1821−24 and 1923−13 are noted as having possibly shown transient VHE emission. The Tata group (Bhat et al. 1990) observed PSR B 0355+54 with positive evidence which could not be confirmed in a later follow-up observation. The Gulmarg group reported evidence on DC flux of PSR B 0355+54 (Senecha et al. 1995), which is, however, an order of magnitude larger than the upper limit to the DC flux obtained by the Whipple group (Reynolds et al. 1993). PSR B 1259−63 (Manchester et al. 1995), in a highly eccentric binary orbit, presents an interesting site for pulsar wind experiments at varying distances between the pulsar and its massive companion. The CANGAROO group observed this object with a preliminary result on the DC flux at the $\sim 4\sigma$ significance level, which encourages repeated observations. The binary pulsar PSR J 0437−47 of 5.8 ms period is interesting because of its distance of only 140 pc. An upper limit for the pulsed flux above 1 TeV of 5×10^{-11} cm^{-2} s^{-1} was reported by Dazeley et al. during this Colloquium.

Among the total 558 pulsars listed in Taylor et al. 1993 there are 48 pulsars with period shorter than 100 ms, including 21 binary pulsars. Only Geminga and six radio pulsars have been found by EGRET to emit high energy gamma rays, with upper limits set for 40 other short period pulsars. The VHE survey with decent observation time is still limited to a small number of pulsars, and all the claims reported so far for detections of non-EGRET pulsars are of marginal significance. Efforts to achieve a more "complete" survey are necessary for arguing about emission models of VHE gamma rays from radio pulsars.

3 Discussion

3.1 Brightness in the VHE gamma ray band

In calculating the luminosity L_{VHE} in the VHE gamma ray band from the reported flux, there are many factors which cause systematic errors; the threshold energy of the observations, the shape of energy spectrum to be integrated, contamination of the background (above which the gamma ray signal is detected), as well as the distance to

Table 2: Observation list on millisecond and binary pulsars

Name	$P^{(*)}$	Flux (cm^{-2} s^{-1})	$E_{th}^{(**)}$	Group
0355+54	156.4	7.9×10^{-12}	1.3	Tata
		$< 5.4 \times 10^{-13}$	3.4	Tata
		4.5×10^{-11}	4 ; DC?	Gulmarg
		$< 4.0 \times 10^{-12}$	0.45; DC	Whipple
0437−47	5.8	$< 5 \times 10^{-11}$	1	BIGRAT
1259−63	47.8	a few times 10^{-12}	3 ; DC	CANGAROO
1821−24	3.1	transient		Potchefstroom
1823−13	101.5	transient		Potchefstroom
1855+09	5.4	4×10^{-10}	0.4	Durham
		$(2.3 \pm 2.5) \times 10^{-10}$	2	Potchefstroom
		$< 9.5 \times 10^{-12}$	0.6 ; DC	Whipple
1937+21	1.5	3×10^{-11}	1	Durham
1953+29	6.1	3×10^{-11}	2	Durham
1957+20	1.6	$< 2.8 \times 10^{-11}$	0.4	Durham

*: Period (ms). **: Threshold energy of detected gamma ray in TeV.

pulsar. Some of these conditions depend on the individual observations, the details of which are not clearly known. Most of the positive results on the millisecond pulsars are of claims for pulsed emission. In this case, there are uncertainties in the beaming factor of the emission angle and the duty cycle against the phase of pulsar rotation. We attempt in this paper to compare the VHE luminosity on a common base for different pulsars. The results plotted in Fig. 1 assume, for all observations, the same photon index of −2.5 and the same energy range of 500 GeV to 10 TeV despite the varying threshold energies from observation to observation. The distances listed in Taylor et al. 1993 are used. The solid angle of emission is taken to be 4π and 1 steradian, respectively for unpulsed and pulsed emission. Some of the luminosities calculated here are considerably different from those given in the papers that reported the observation, which is not surprising in view of the existing uncertainties. In Fig. 1, the horizontal axis is log (L_{sd}/d^2) in units of erg s^{-1} cm^{-2}, where d is the distance to the earth, and the vertical axis is log η, where η is the ratio of gamma ray luminosity to spin down luminosity L_{sd}. The VHE luminosity is used for unfilled symbols ($\eta = L_{VHE}/L_{sd}$), and the luminosity in 100 MeV to 30 GeV is used (instead of L_{VHE}) for EGRET pulsars, which are shown with a black circle. Data of a same flux at the earth will appear in parallel with the dotted line which represents L_{VHE}/d^2 = constant.

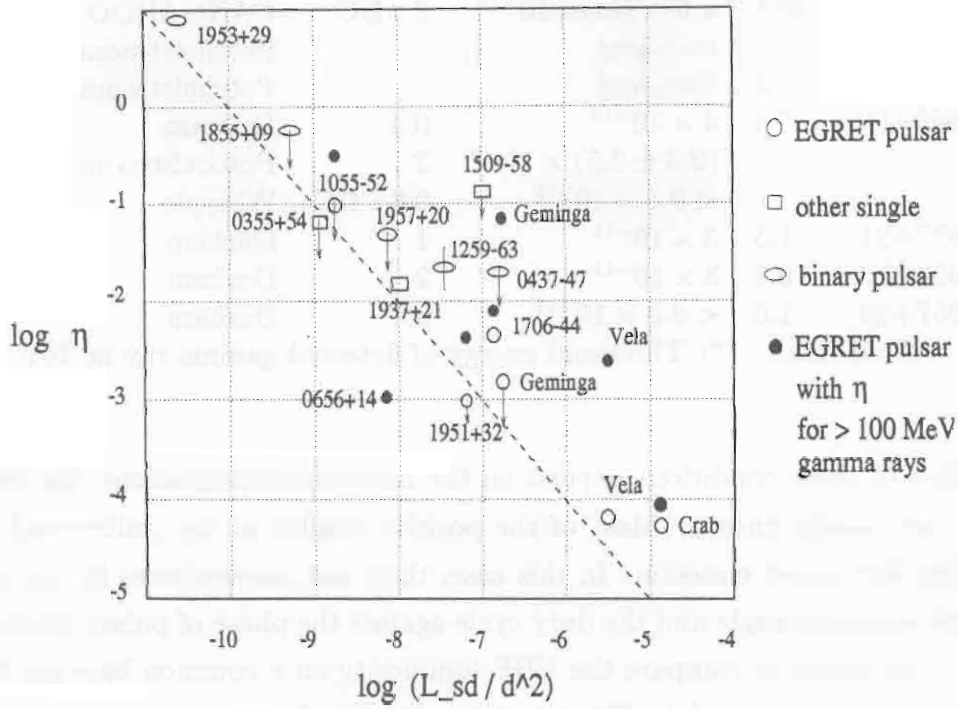

Figure 1: Scatter plot of brightness in VHE gamma rays and rotational energy loss of pulsars.

3.2 Relation to other energy bands

It appears that VHE emission from the EGRET pulsars is unpulsed: not modulated with pulsar period. This fact indicates that the VHE emission is not from the pulsar magnetosphere but from a remote site where pulsar wind collides with circumstellar matter. The VHE fluxes from the Crab, PSR B 1706−44 and Vela correspond to luminosities of $\sim 2 \times 10^{34}$, $10^{33} \sim 10^{34}$, and $10^{32} \sim 10^{33}$ erg s^{-1}, respectively. For the latter two objects, the calculated value has an uncertainty of almost an order of magnitude depending on the power index and cutoff energy of the spectrum. With this in mind, by assuming that VHE gamma rays and X-ray emission are from inverse Compton and synchrotron processes respectively, we can estimate the magnetic field by comparing the VHE and X-ray luminosities. The smaller X-ray luminosities than that of the Crab nebula yield weaker magnetic fields of $1 \sim 10\mu$G for PSR B 1706−44 and the Vela pulsar.

For the Vela pulsar, which is at a distance of only ~500 pc, it is useful to know the geometrical structure of emission mechanism. The complex structure in the vicinity of Vela pulsar appears from X-ray data; the existence of a point-like source at the pulsar, a $4'$ nebula of diffuse emission, and hard X-ray emission extending from the pulsar to the radio feature Vela X (Harnden et al. 1985); soft X-ray emission extending from the pulsar towards the south can be the result of non-thermal interactions by the pulsar wind (Markwardt and Ögelman 1995), of which strong evidence would be given by gamma ray detection.

It is interesting to speculate on what type of pulsars would be bright at VHE gamma ray energies; pulsars which have accompanying synchrotron X-ray emission are likely VHE sources because of the existence of energetic electrons. Particle acceleration may take place at the shock generated by the pulsar wind that carries most of the rotational energy loss of the neutron star. The X-ray satellites ROSAT and ASCA are recently increasing the number of X-ray synchrotron nebula and/or pulsar wind sources. Also in this Colloquium, evidence of a pulsar wind was presented by N. Kawai from the ASCA group in a report of elongated emission bridging the synchrotron nebula of MSH 15−52 and the pulsar PSR B 1509−58. The upper limit of VHE gamma rays reported for this object is not very stringent and a flux larger than the current sensitivity of imaging Čerenkov telescopes is estimated by du Plessis et al. (1995).

Less intense synchrotron X-rays are expected from lower magnetic fields (if the energy and number of progenitor electrons are kept constant) while more intense VHE gamma rays relative to the X-ray intensity are expected. However, with low magnetic fields, the characteristic wavelength of synchrotron radiation can be in the UV to softer X-ray region, lower than the ROSAT and ASCA bands. In some pulsars, the energy

spectrum of progenitor electrons can be steep, without continuing to high enough energy to produce detectable VHE emission. Thus, the existing X-ray and VHE gamma ray data are not good enough to allow detailed comparisons. The next generation of VHE telescopes is eagerly awaited, as these will be operating at energies lower than the current threshold of several hundred GeV.

3.3 Transient emission and Imaging technique of Čerenkov light

The high η values of some millisecond pulsars (Fig. 1) can suggest a very efficient mechanism of VHE emission and particle acceleration process. Similar results have been reported for on accretion-powered X-ray pulsars (Chadwick et al. 1990). Repeated observations are needed to resolve these puzzles. Difficulty in confirming the earlier results is due to the fact that most of the detections were obtained at a time of a burst-like increase of observed events which could enhance the significance of the time-correlated signal with the pulsar period. With imaging Čerenkov telescopes, however, a transient burst will appear as an increase of events with gamma ray-like features (i.e. in the imaging parameters such as the orientation angle α) while cosmic ray background events can be monitored to ensure they stay constant with time. Imaging Čerenkov technique observations of such transient phenomena will be very useful for examining the time-varying characteristics of such sources.

4 Conclusions and Summary

The ratio η of the scatter plot in Fig. 1 appears at the $\sim 10^{-4}$ level for 'DC' emission of VHE gamma rays from the Crab and Vela pulsars, while of the order of 10^{-3} for PSR B 1706−44. Pulsed VHE emission has not been detected at a high confidence level for any of the EGRET pulsars, and the ratio is likely to be considerably smaller than the unpulsed case. There are interesting differences in the observational data among the three pulsars, Crab, Vela and PSR B 1706−44. We need more data to compare more pulsars. The dissimilarities must be related to the different conditions of VHE emission in the pulsars.

The observed values and upper limits of the ratio η are considerably larger for some pulsars than those of the Crab and Vela. A similar tendency of large η and variations from pulsar to pulsar can be seen among the EGRET detections, as shown by the filled circles in Fig. 1. Pulsars with accompanying X-ray emission, such as PSR B 1509−58, are worth extensive VHE observations. Binary pulsars such as PSR B 1957+20 and 1259−63 can be bright in VHE gamma rays due to the interaction of the pulsar wind

with a close companion star. The 500 pc distance to the Vela pulsar means that the typical angular resolution of an imaging Čerenkov telescope, 0.1°, corresponds to about 1 pc at the source, which is not far from the size of pulsar wind shock of 0.1∼1 pc in the case of Crab (Kennel and Coroniti 1984). If the pulsar wind causes non-thermal phenomena resulting in the emission of gamma rays in a close binary system like PSR B 1259−63, the site of such a process is within $\sim 10^{13}$ cm from the pulsar, much less than the ~ 0.1 pc of the Crab. It is thus hoped that a more complete survey in VHE gamma rays of various types of pulsars will reveal interesting information on the behaviour of the pulsar wind such as the shock distance and strength of the magnetic field generated by pulsar wind.

The dotted line in Fig. 1 corresponds to a VHE gamma ray flux, 1.5×10^{-12} cm^{-2} s^{-1}, for photons >1 TeV, which is roughly equal to the current sensitivity of imaging Čerenkov telescopes. The VHE data points in Fig. 1 are distributed almost along the dotted line, suggesting that the plotted data are influenced by detection biases and raising the hope that more sources may appear with continued efforts.

Acknowledgements

Thanks to P.G. Edwards for reading the manuscript and for comments and to the VHE colleagues who kindly informed the author of their latest results.

References

Aharonian, F.A. and Atoyan, A.M., 1995, Astroparticle Phys. 3, 275
Akerlof, C.W. et al. 1993, A&A, 274, L17
Bhat, P.N. et al. 1987, A&A, 178, 242
Bhat, P.N. et al. 1990, A&A, 236, L1
Borione, A. et al. 1995, Proc. 24th Int. Cosmic Ray Conf., 2, 350
Bowden, C.G.G. et al. 1990, Nuclear Phys. B(Proc. Suppl.) 14A, 75
Bowden, C.G.G. et al. 1993a, Proc. 23rd Int. Cosmic Ray Conf., 1, 294
Bowden, C.G.G. et al. 1993b, J. Phys. G., 19, L29
Brink, C. et al. 1990, ApJ, 346, L37
Brink, C. et al. 1993, 23rd Proc. Int. Cosmic Ray Conf., 1, 334
Cawley, M.F. and Weekes, T.C. 1995, Exp. Astron., 6, 742
Chadwick, P.M. et al. 1985, Nature, 310, 236
Chadwick, P.M., McComb, T.J.L. and Turver, K.E. 1990, J. Phys. G., 16, 1773
Cheng, K.S., and de Jager, O.C. 1990, Nuclear Phys. B(Proc. Suppl.), 14A, 28
Djannati-Atai, A. et al. 1995, Proc. 24th Int. Cosmic Ray Conf., 2, 315
Dowthwaite, T.C. et al. 1984, ApJ, 286, L35
du Plessis, I. et al. 1995, ApJ, 453, 746

Edwards, P.G. et al. 1994, A&A, 291, 468
Gillanders, G.H. et al. 1995, Proc. 24th Int. Cosmic Ray Conf., 2, 323
Goret, P. et al. 1993, A&A, 270, 401
Grindlay, J.E. et al, 1975, ApJ, 201, 82
Harnden, F.R. et al, 1985, ApJ, 299, 828
Kalekin, O.G. et al. 1995, Astron. Lett., 21, 163
Kennel, C.F. and Coroniti, F.V. 1984, ApJ, 283, 710
Kifune, T. et al. 1995, ApJ, 438, L91
Konopelko, A. et al. 1995, preprint MPIK-K-33-1995
Lewis, D.A. et al. 1993, Proc. 23rd Int. Cosmic Ray Conf., 1, 279
Manchester, R.N. et al. 1995, ApJ, 445, L137
Markwardt, C.B. and Ögelman, H. 1995, Nature, 375, 40
Nel, H.I. et al. 1992, ApJ, 398, 602
Nel, H.I. et al. 1993, ApJ, 418, 836
Ramanamurthy, P.V. et al. 1995, ApJ, 447, L109
Ramanamurthy, P.V. et al. 1996, ApJ, 458, 755
Reynolds, P.T. et al. 1993, ApJ, 404, 206
Sapru, M.L. et al. 1996, Bull. Astr. Soc. India, in press
Senecha, V.K. et al. 1995, A&A, 302, 133
Tanimori, T. et al. 1994, ApJ, 429, L61
Taylor, J.H., Manchester, R.N., and Lyne, A.G. 1993, ApJ, Suppl. 88, 529
Vishwanath, P.R. et al. 1993, A&A, 267, L5
Vishwanath, P.R. et al. 1994, *Towards a Major Atmospheric Čerenkov Detector* (Ed. T. Kifune, Academic Press, Tokyo), 65
Weekes, T.C. 1996, personal communication

Recent Status of Next CANGAROO Project of Air Čerenkov Imaging Telescope for sub-hundred GeV Gamma-Ray Detection

CANGAROO Collaboration

Presented by T.Tanimori

Department of Physics, Tokyo Institute of Technology, Tokyo 152, Japan

Abstract

The CANGAROO group attempts to exploit sub-hundred GeV region for gamma-ray astronomy by constructing a new imaging Air Čerenkov telescope of large aperture, scheduled to be installed at Woomera, South Australia, in 1998. We begin with a light collection area equivalent to 7m diameter, which consists of ~40 spherical mirrors of 0.8m diameter. The reflector area is to be enlarged to 10m diameter by adding 40 more spherical mirrors. The design study on photomultiplier tube camera and readout system have been almost finished and is presented in this paper. Also discussed are several problems in achieving measurement of sub-hundred GeV gamma-rays, and new technical ideas to improve sensitivity.

1. Introduction

The necessity of a large sized Imaging Air Čerenkov Telescope (IACT) of 10m class, in order to exploit the new window for observing high energy γ-rays less than 100 GeV, can not be overemphasized, and, to date, the feasibility of constructing such a telscope has been discussed and examined in the CANGAROO group (Kifune & Tanimori 1993; Tanimori et al. 1994). Soon after the Tokyo workshop "Towards a Major Atmospheric Čerenkov Detector-III" held in May 1994, our proposal of constructing a new large IACT at Woomera in South Australia was fortunately approved (Cangaroo-II project) by a four years' funding until 1998 fiscal year. The construction of the main body of the telescope will be over one year before the end of the funding, and the installation and test operation will be done during the fiscal year of 1998.

There can be many different ways along which we develope the current technique of the ground based gamma ray astronomy. However, our strategy is to fill the observation gap that exists at sub-hundred GeV energies above the satellite detection (currently up to 30 GeV). For this purpose, we need to reduce the energy threshold of detectable gamma rays, which will enable us to discover more number of sources of very high energy gamma-rays and also provide useful information on energy spectrum and energy dependence of time structure of the signal from pulsars, *i.e.* pulsed or unpulsed.

Almost all the gamma-ray spectra observed such as from pulsars and AGN (Active Galactic Nuclei) detected by the EGRET detector of CGRO (Compton Gamma Ray Observatory) extend beyond 10 GeV (Montigny et al. 1995), while only a few gamma-ray sources have been detected so far above 200 GeV by IACTs. There should exist energy cutoff at the sub-hundred energies in the gamma-ray emission from almost all the pulsars and AGN. Detection of the cutoff energy is related to important information to understand the mechanism of gamma-ray production and, about AGN, propagation of gamma-rays in the the extragalactic space (e.g., Stecker, de Jager & Salamon 1992).

We construct a telescope of which frame and base can sustain a large collection area of a 10m diameter mirror. A detailed cost estimate allows us to prepare only a half area of the mirror in the beginning stage and with more fund available later, the light collection area will be easily extended to a 10m diameter by the attachment of composite small mirrors to the frame of the telescope. We use an already existing design of 10m radio antenna and the cost is similar to that which would be necessary to newly design a 7m telescope.

In the followings, we describe the design concepts of our telescope, camera and readout system, which are required to detect Čerenkov light image generated by sub-hundred gamma-rays.

2. Design of Mirror

At the time of commencing very high energy gamma-ray astronomy in sub-hundred GeV region, most important points are the large area of reflector to collect as many as Čerenkov photons as possible. We need to make every effort for as good qualities of focusing lights as possible, *i.e.* to optimize the design for efficiently concentrating reflected Čerenkov photons into as small number of pixels of the camera as possible. An optical or a radio telescope is usually designed to have very sharp image of point source only within a narrow FOV of a few arcminutes using a Cassegrain mirror by which the coma aberration can be easily canceled out. Thus, the requirements for Air Čerenkov telescope are quite different from those for optical or radio telescopes. Čerenkov lights from air shower has extended feature, larger than ~0.1 degree, and a blur around this size is tolerable. However, the size of the blur should not vary largely over a wide field of view (FOV) of at least about 3 degrees across.

Spherical mirrors have been so far adopted as an Air Čerenkov mirror by many existing groups. A spherical mirror in principle has "quasi-focusing" characteristics due to aberration, with about a few tens % of photons incident in parallel reflected and focused to hit one pixel of the phototube camera. As one kind of composite systems of many small spherical mirrors, the David-Cotton type has been adopted for the use of

IACT (e.g. Whipple and CAT groups). It can improve the large amount of aberration in a spherical morror down to as small as that with a parabolic mirror. However, the spherical mirror such as the David-Cotton type results in a large spread of arrival times of collected photons. The path length of each photon arriving in the focal plain varies as a function of the reflection points on the mirror in the case of a spherical mirror, while kept constant for a parabolic mirror. In order to decrease the energy threshold, Night Sky Background (NSB) has to be rejected as much as possible. NSB can be removed from Čerenkov photons by a narrow gate width which is possibly shortened to 10ns, Therefore the narrow gate can be applied efficiently only to a parabolic mirror. We attempt to decrease the energy threshold below 100 GeV by using a parabolic mirror, as will be described in the section 4.

A composite system of mirrors has merits; easier construction by assembling many small mirrors; a dramatic reduction in the cost. We designed a 10 m diameter parabolic mirror which consists of about 80 small spherical mirrors of a 80cm diameter. The allignment of the small mirror is explained in Fig.1. The hatched region is to be covered later for increasing an area from the beginning 7m to 10m diameter.

The size of coma aberration is strongly dependent on a chosen value of the focal length of a parabolic mirror. The fact that the imaging Čerenkov technique needs a large FOV implies that a good focusing is required in the outer part near the edge of FOV as well as in the center of FOV. In general, a longer local length provides with smaller aberration, while deformation of the mirror, due to the gravity, however, grows with increasing focal length. We have chosen 8m as the focal length, with which the deformation is tolerable and we expect a reasonably small coma aberration at 1 degree distance from the center of FOV. In principle, a parabolic mirror causes a larger coma aberration for the photons incident with larger angles to the light axis. Another merit of a composite mirror is that the radius of curvature of each small spherical mirrors can be determined independently to improve the aberration. We searched for the optimum condition by Monte Carlo simulation, and found that the best solution is with the radius of curvature of small mirrors to be 1640cm, when the focal length is 800cm. Figure 2 shows the simulated alpha distributions for gamma-rays of various energies for a parabolic composite mirror of 7m and 10m aperture with the above value of radius of curvature. We expect to achieve $\sim$ 80 GeV energy threshold in the first stage with 7m aperture and 50 GeV with 10m telescope. The details of the Monte Carlo study for the optical design of this telescope and the expected performance are reported by Hayami in this Workshop.

We attempt to use plastic mirrors. Most of mirrors of air Čerenkov telescope have been so far made of glass (some are of metal), since the material is easier to obtain good

reflection and fine image. However, the glass is fragile and relatively heavy, and, in the Čerenkov telescope for gamma ray astronomy, we don't need as fine image as those in optical astronomy. The plastics, on the other hand, is less rigid, which is the main reason for not in use. Recently, however, Carbon Fiber Reinforced Plastic (CFRP) has been applied to various technological areas because of its distinctive features of hardness, lightness and easiness of forming any requested shapes. Thus, we challenge to use CFRP as a material of a small spherical mirror. For the protection of the mirror, fluorine oxide is coated on the aluminum surface put onto CFRP. The reflectivity of a prototype mirror was measured to be 82% and efforts for further improvements are in progress.

3. Camera & Readout System

The camera will consist of ~550 small photomultiplier tubes (PMT) of 13mmϕ (Hamamatsu R4124) to cover a total field of view of about 3° across. The photocathode of each PMT has an area of 10mmϕ, corresponding to 0°.12ϕ, implying that the photo-sensitive area covers ~ 40% of the total field of view. In order to increase the sensitive area of the camera, an array of light collectors will be attached in front of phototubes. A prototype of the light collector has been tested by installing with the existing 3.8m CANGAROO telescope. The prototype one has a truncated pyramidal shape of 18mm length with 12mm×12mm front face and 7mm×7mm back face, of which inside surface is coated with nickel. The shape was designed through simulation calculation to optimize the light collection efficiency of the 3.8m CANGAROO telescope. Although a hollow type of the light collector is susceptible to deterioration of collection power of photons compared with the block type of light guide used in HEGRA group (Wiedner 1995), the hollow type is free from the effect of cosmic ray muons travelling through the light guide material, which yields a considerable amount of Čerenkov lights, giving similar signals to gamma-ray images.

The PMT we use has a good peak of single photo-electron as well as a small timing jitter of ~ 0.7ns for one photo-electron. As will be discussed in detail in the next section, the timing information is a key factor to reduce the energy threshold below 100 GeV. Sixteen PMTs are installed in one module box (PMT module) with a common bleeder circuit for PMTs, and buffer amplifiers to feed signals through twisted pair cables to a curcuit of trigger modules. In order to avoid possible gain variations caused by exposure to NSB light, the PMTs are operated with low gain of ~ 10^5, and the last four dynode stages of ten dynodes in R4124 are sustained by a common transistor base in a PMT module. Signals from PMTs are then multiplied by ~100 using monolithic amplifiers (LeCroy TRA402), and the total gain in PMT module is determined to be ~ 10^7.

Figure 3 shows the schematic diagram of the readout system. In order to process the output pulses from PMTs, we use a "Trigger Module" based on the "TKO specification" which was developed by KEK (National Laboratory for High Energy Physics in Japan). Each module has 32 inputs and contains main amplifiers (gain of factor 5), high threshold and low threshold discriminators, scalers, and summing circuits for obtaining both the number of "hit" PMTs and the total sum of pulse heights from one PMT module. In the Trigger Module, each signal is fed to both the low and high threshold discriminators; the former discriminates a signal at ~two photo-electrons level with an output pulse of the same width with the input signal. The latter generates a discriminated pulse at ~four photo-electrons of which width is fixed to be ~10ns and used for trigger pulse. The number of "hit" phototubes in one PMT module is obtained by summing all the currents of the output pulses of the high level discriminators. In addition, the discriminated pulse of each PMT is independently counted by a scaler in 1 ms duration time (recorded at every event trigger), for monitoring the amount of NSB, bright stars in FOV and the stability of each PMT. An analog pulse of each PMT is also added together in a common module of sixteen PMTs in order to generate a "clustering trigger" which selects an event of Čerenkov photons concentrated into a few neighboring PMTs.

Each pulse after the low level discriminator is fed to CAMAC Multi-hit TDC (LeCroy 3377) by which we measure both the arrival time and the pulse width simultaneously. Since the pulse width is proportional to the logarithm of the pulse height, the TDC informations provide us with both the timing and the number of incident photons in individual PMTs. This procedure of measuring deposited electric charge through the pulse width has been used for relatively slow pulses. In some of the experiments of such as extensive air shower detectors, a pulse of PMT is expanded by shaping amplifiers with a few μs and the width measured by a clock counter. Ours is "advanced" from these traditional ones in a point that we use a fast clock of 0.5ns and multi-hit recording. The minimum width measured in the TDC of Le Croy 3377 is 10ns which corresponds to the gate width of ADC. The width of the smallest pulse from the amplifier for one photoelectron is adjusted to 10ns. We have to deal with a small number of Cerenkov photons in one PMT, and the number can be comparable with a few photons of NSB. In such a case, it is possible to reduce the gate width for small signals less than 10 ns, *ad hoc* by software, by using the TDC data of arrival time of photons. For large pulse heights, the pulse width increases logarithmically, which may cause NSB photons to accidentally contaminate the pulse. However, the effect is not serious because the number of Čerenkov photons generating a wide pulse is relatively large. Figure 4 shows the relation of the charge measured by ADC and the pulse width measured by TDC.

Since the pulse width corresponds to the logarithm of pulse height, the part in smaller values appears almost linear, and tends to gradually deviate from the linear relation at higher values. We have obtained a fitting function of the relation, and simulated the performance of gamma ray detection with the 10m telescope by using the fitting function. There were found no serious effects such as temparature dependence during a long time operation of this method.

The data of "hit" phototubes are read from each TDC, and sent to MicroSparc Workstation through both VME-CAMAC interface and VME-S-bus interface (Takeuchi et al 1993). The typical data size and trigger rate are expected to be ~200 byte per event and ~30Hz, respectively. The rate of data transfer is roughly 6kB/s, and the dead time due to the data acquisition is estimated to be less than a few percent. We can also adopt a clustering trigger using the summed output from each PMT module to reduce the effect of NSB for the trigger counting rate.

4. Further Improvements

Recently the Whipple group reported that the single cosmic ray muon leads to a major background in detecting 200 GeV gamma-rays (Catanese 1995). Our simulation study also indicates that the cosmic ray muons causes a serious effect of mimicing gamma-like events. Cosmic ray muons which hit the area within several tens of meters from the telescope tend to satisfy the triggering conditions with increasing area of light collection of large aperture IACT, and the faint but sharp and elongated shapes of Čerenkov light image can be hardly distinguished from gamma ray events by applying the ordinary imaging analysis. However, single cosmic ray muons and air shower events have dissimilar structures in their arrival times of Čerenkov photons. With a fine timing resolution of less than 1ns, we expect that the image generated from cosmic ray muons can be removed without losing almost all the gamma-ray events. In order to achieve such a timing resolution, we need TDC data for Čerenkov photons which shoud be collected by a parabolic mirror (see for the details a brief talk presented by Hayami in this conference and also the one by Tanimori and Hayami which will appear elsewhere). Thus, we prefer a parabolic mirror as a next generation of IACT to the David-Cotton type of spherical composite mirror.

In addition, it is also noted that the parabolic mirror may add another important benefit to the imaging Čerenkov technique. A lense system can be installed to reduce the coma aberration, while the mirror of the David Cotton type loses the phase information. The coma aberration in the outer part of FOV ($\theta \geq 1^{\circ}.2$) is estimated to be ~3cm which is almost twice of our pixel size. In general, the coma abberations is known to be diminished by installing a combination of two or three compensation lenses. Even one

compensation lense located at 70cm in front of the camera reduces the size of aberration to less than 1cm for an "ideal" (not a composite of small mirrors but one dish) 10 m parabolic mirror, as shown in Fig.5. We estimated by simulation calculation the yield of photon hitting one PMT with one compensating lens inserted for our 10m composite mirror, and Figure 6 shows the ratio of the yield with the lense to that without the lense as a function of the distance of the concerned PMT from the center of FOV. It is noted that the figure of merit by the use of one compensating lens is close to twice in the outer region of FOV which occupies about a half of the total detection area, although the effect of the lense is largely reduced for the composite mirror compared with the case of the "ideal" parabolic mirror. In the simulation, we assumed to use the acrylic as a material of the lense to reduce the weight. Investigations by simulation study are now underway in Tokyo Instiute of Technology and Ibaraki University.

The project is funded by A Grant-in-Aid for Scientific Research, The Ministry of Education, Science, Sports and Culture, as one of the Fields of Priority, "Very High Energy Astrophysics". We thank Mitsubishi Electric Company for the assistance in the design and construction work of the main body of the telescope.

References

1. Catanese, M., et al. 1995, in Proc. 4th Internat. Workshop "Towards a Major Atmospheric Čerenkov Detector"(Padova), 335.

2. Kifune, T., & Tanimori, T. 1993, in Proc. 2nd Internat. Workshop "Towards a Major Atmospheric Cerenkov Detector"(Calgary), 243.

3. Montigny, C., et al. 1995, ApJ, 440, 525.

4. Stecker, F.W., de Jager, O.C., & Salamon, M.H., 1992, ApJ, 390, L49.

5. Tanimori, T., et al. 1994, in Proc. 3rd Internat. Workshop "Towards a Major Atmospheric Cerenkov Detector"(Tokyo), 311.

6. Tanimori, T., and Hayami. 1996, in preparation.

7. Takeuchi, Y., Tanimori,T., and Yasu, Y. 1993, Nucl. Instr. and Meth., A328, 526.

8. Wiedner, C. A., 1994, in Proc. 3rd Internat. Workshop "Towards a Major Atmospheric Cerenkov Detector"(Tokyo), 119.

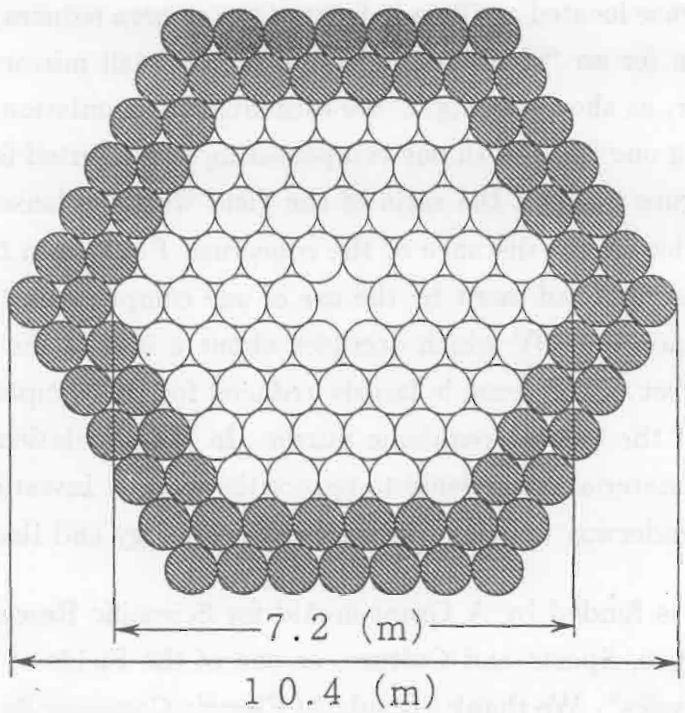

Figure 1: Front view of the next Cangaroo mirror, where hatched region is the additional part for a extension to the 10m diameter mirror, and will be attached a few years later.

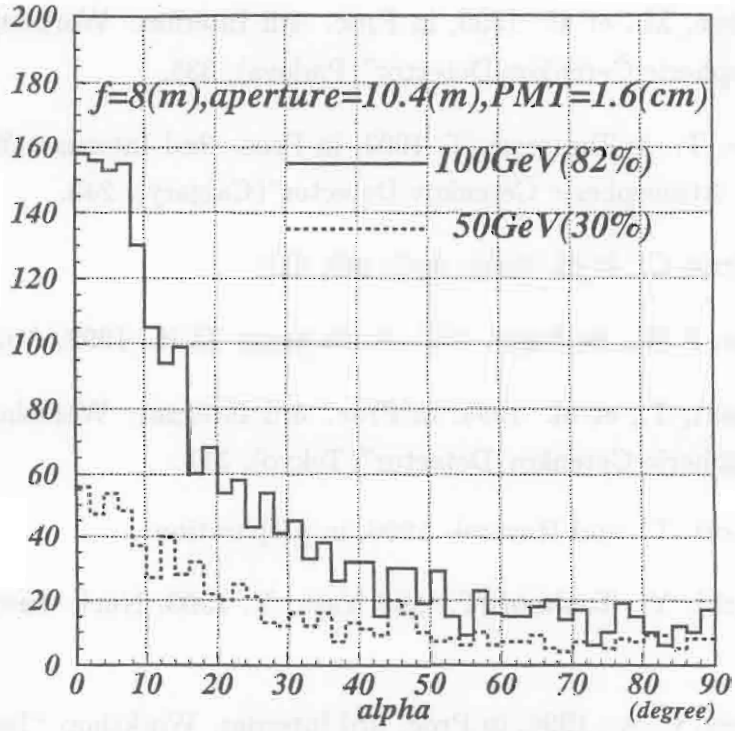

Figure 2: Simulated alpha distributions for various energetic gamma-rays for both a 7m and a 10m diameter parabolic mirrors consisting of 80cmϕ spherical mirrors, where the detection efficiency are also calculated.

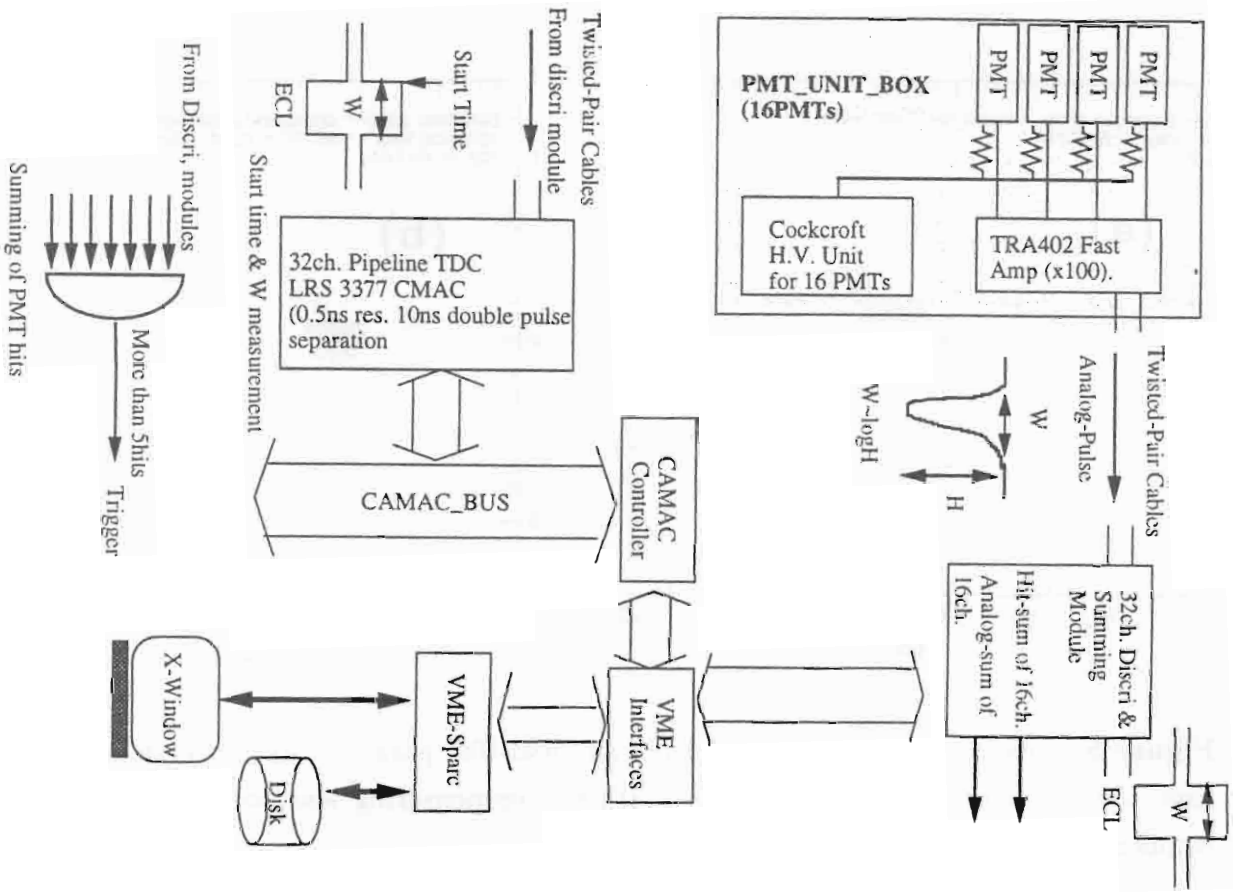

Figure 3: Schematic diagram of the readout system.

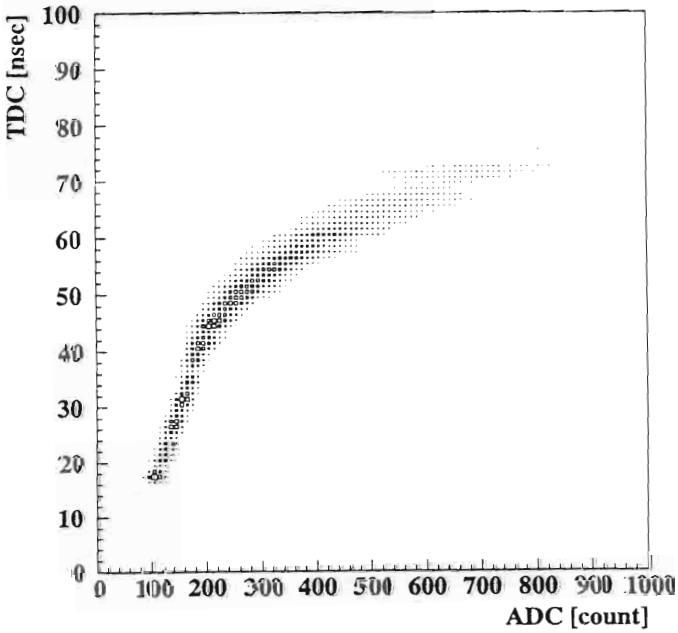

Figure 4: Relation of charge measured by ADC and the pulse width measured by TDC. Since pulse width corresponds to the logarithm of the pulse height, the part in smaller value looks to be almost linear, but that in higher value gradually deviates from linear relation.

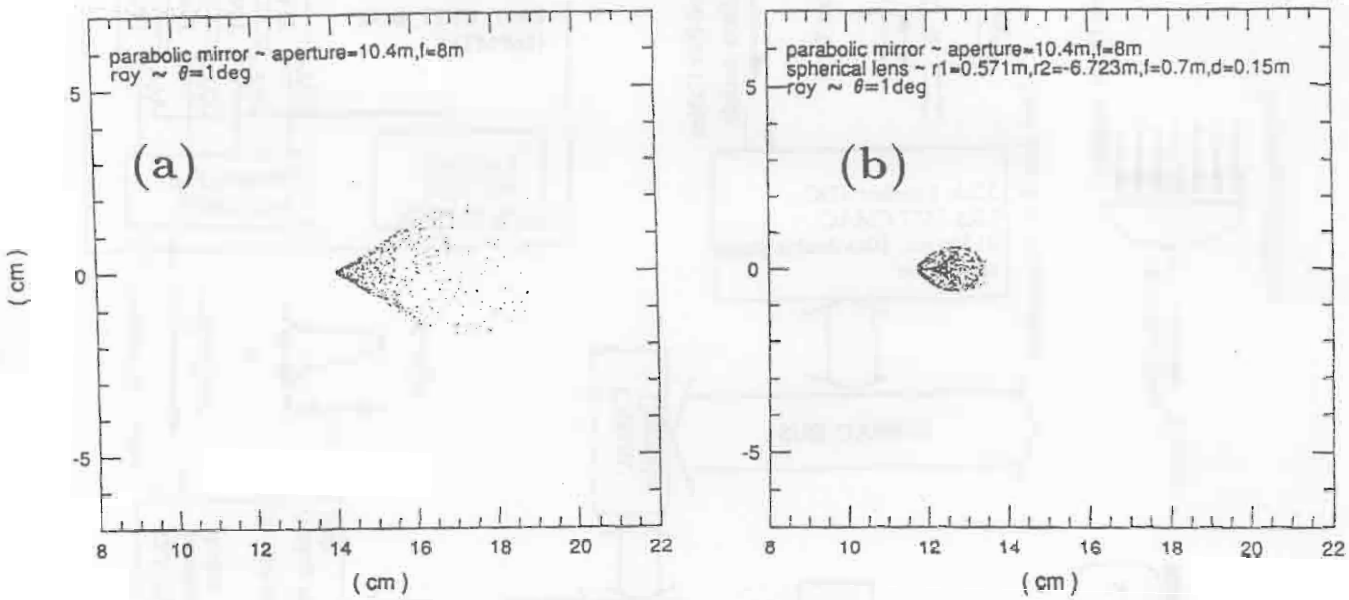

Figure 5: Simulated Coma abberations of an ideal 10m parabolic mirror at ($\theta \geq 1°.2$) from the center of the field of view (a) with no compensating lens, and (b) with one compensating lens.

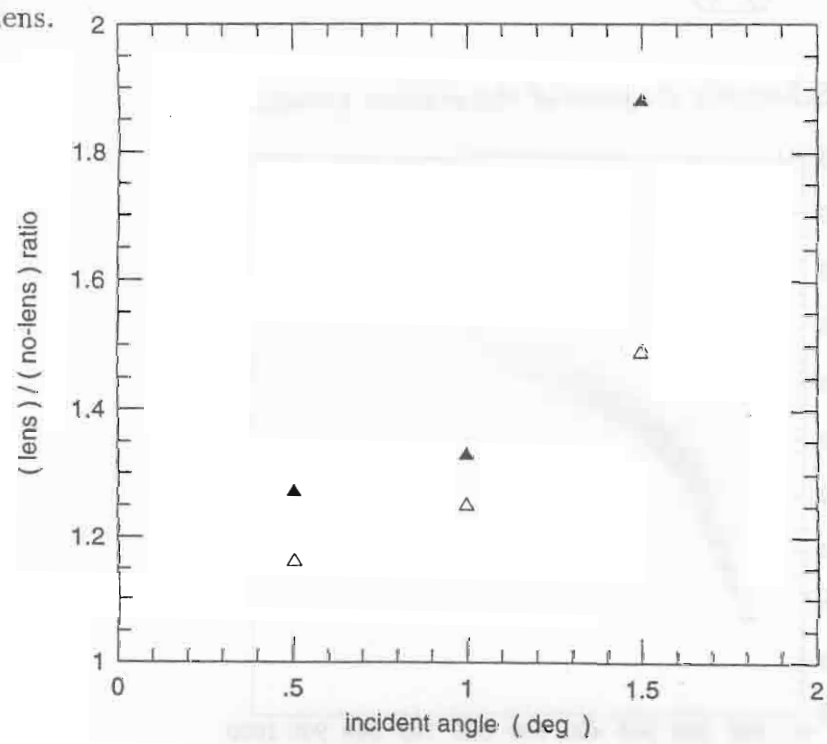

Figure 6: Simulated ratio of the yield of photon on one phototube (10mm square size →open triangle; 15mm square size →black triangle) with one compensating lens to that without it for our 10m composite mirror as a function of the distance from the center of the field of view.